Langmuir

Article

pubs.acs.org/Langmuir

Supramolecular Composite Materials from Cellulose, Chitosan, and Cyclodextrin: Facile Preparation and Their Selective Inclusion Complex Formation with Endocrine Disruptors

Simon Duri and Chieu D. Tran*

Department of Chemistry, Marquette University, P.O. Box 1881, Milwaukee, Wisconsin 53201, United States

Supporting Information

ABSTRACT: We have successfully developed a simple one-step method of preparing high-performance supramolecular polysaccharide composites from cellulose (CEL), chitosan (CS), and (2,3,6-tri-*O*-acetyl)-α-, β-, and γ-cyclodextrin (α-, β-, and γ-TCD). In this method, [BMIm$^+$Cl$^-$], an ionic liquid (IL), was used as a solvent to dissolve and prepare the composites. Because a majority (>88%) of the IL used was recovered for reuse, the method is recyclable. XRD, FT-IR, NIR, and SEM were used to monitor the dissolution process and to confirm that the polysaccharides were regenerated without any chemical modifications. It was found that unique properties of each component including superior mechanical properties (from CEL), excellent adsorption for pollutants and toxins (from CS), and size/structure selectivity through inclusion complex formation (from TCDs) remain intact in the composites. Specifically, the results from kinetics and adsorption isotherms show that whereas CS-based composites can effectively adsorb the endocrine disruptors (polychlrophenols, bisphenol A), their adsorption is independent of the size and structure of the analytes. Conversely, the adsorption by γ-TCD-based composites exhibits a strong dependence on the size and structure of the analytes. For example, whereas all three TCD-based composites (i.e., α-, β-, and γ-TCD) can effectively adsorb 2-, 3-, and 4-chlorophenol, only the γ-TCD-based composite can adsorb analytes with bulky groups including 3,4-dichloro- and 2,4,5-trichlorophenol. Furthermore, the equilibrium sorption capacities for the analytes with bulky groups by the γ-TCD-based composite are much higher than those by CS-based composites. Together, these results indicate that the γ-TCD-based composite with its relatively larger cavity size can readily form inclusion complexes with analytes with bulky groups, and through inclusion complex formation, it can strongly adsorb many more analytes and has a size/structure selectivity compared to that of CS-based composites that can adsorb the analyte only by surface adsorption.

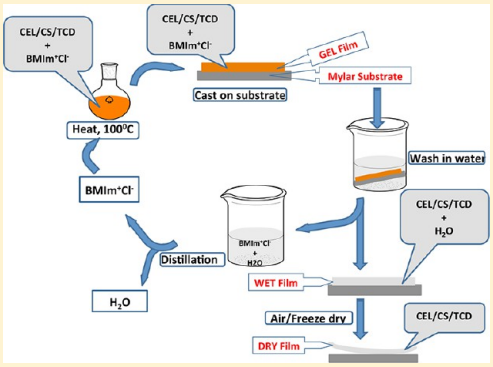

1. INTRODUCTION

Supramolecular composite material is an organized, complex entity that is created from the association of two or more chemical species held together by intermolecular forces.[1−5] Its structure is the result of not only additive but also cooperative interactions, and its properties are often better than the sum of the properties of each individual component.[1−3] Supramolecular composite materials containing marcrocyclic polysaccharides such as cyclodextrins (CDs) are of particular interest because CDs (α-, β-, and γ-CD) are known to form selective inclusion complexes with a variety of different compounds with different sizes and shapes.[4−6] To be able to utilize properties of the CD-based supramolecular composite material fully and practically, it is necessary for the materials to be readily fabricated in solid form (film and/or particle) in which encapsulated CDs fully retain their unique properties. CDs are very soluble in water and cannot be processed in film because of their poor mechanical and rheological strength. As a consequence, it is often necessary to react and/or graft CD chemically onto man-made polymers to increase its mechanical strength so that the resultant materials can be processed into a solid thin film and/or particles.[7−10] CD-based materials synthesized by these methods have been reported. Unfortunately, in spite of their potentials, practical applications of such materials are rather limited because in addition to the complexity of reactions used in the synthesis that are limited to persons with synthesis expertise, the method used may also alter and/or lessen the desired properties of CDs.[7,8,11,12] It is therefore desirable to improve the mechanical strength of CD-based supramolecular material so that it can be fabricated into a solid film (or particles) not by chemical modification with synthetic chemicals and/or polymers but rather by the use of naturally occurring polysaccharides such as cellulose and/or chitosan, which are structurally similar to CDs.

Cellulose (CEL) and chitosan (CS) are two of the most abundant biorenewable biopolymers on the earth. The latter is derived by the N-deacetylation of chitin, which is the second most abundant naturally occurring polysaccharide found in the

Received: December 17, 2012
Revised: March 14, 2013
Published: March 21, 2013

dx.doi.org/10.1021/la3050016 | *Langmuir* 2013, 29, 5037−5049

exoskeletons of crustaceans such as crabs and shrimp. In these polysaccharides, an extensive network of intra- and interhydrogen bonds enables them to adopt an ordered structure. Although such structure is responsible for CEL having superior mechanical strength and CS exhibiting remarkable properties such as hemostasis, wound healing, bactericide and fungicide, drug delivery, and adsorption for organic and inorganic pollutants, it also makes them insoluble in most solvents.[9,10,13−18] This is rather unfortunate because with their superior mechanical strength and unique properties CEL and CS would be excellent supporting polymers for CD. It is expected that the resulting (CEL and/or CS + CD) composite would have properties that are a combination of those of all of its components. That is, it may have superior mechanical strength (from CEL) and can stop bleeding, heal wounds, kill bacteria, deliver drugs (from CS), and selectively form inclusion complexes with a wide variety of compounds of different types, sizes, and shapes (from CDs). Unfortunately, to date, such supermolecules have not been realized because of the lack of a suitable solvent that can dissolve all three compounds. The difficulty stems from the fact that whereas CDs are water-soluble CEL and CS are insoluble in most solvents. Furthermore, there is not a solvent or system of solvents that can dissolve CEL, CS, and CD.

Considerable effort has been expended in the past few years to find suitable solvents for CEL and CS, and several solvent systems have been reported.[19,20] For example, high temperature and a strong exotic solvent such as methylmorpholine-*N*-oxide, dimethylthexylsilyl chloride, or LiCl in dimethylacetamide (DMAc) are needed to dissolve CEL whereas an acid such as acetic acid is required to protonate the amino groups of CS so that it can dissolve in water.[6−29] These methods are undesirable because they are based on the use of corrosive and volatile solvents, require high temperature, and suffer from side reactions and impurities that may lead to changes in the structure and properties of the polysaccharides. More importantly, it is not possible to use a single solvent or system of solvents to dissolve both CEL and CS. A new method that can effectively dissolve CS, CEL, and CD not at high temperature and not with corrosive and volatile solvents but rather by recyclable "green" solvent is particularly needed. This is because such a method would facilitate the preparation of [CS + CD] and [CEL + CD] composite materials that are not only biocompatible but also have the combined properties of its components.

Recently, we have developed a new method that can offer a solution to this problem.[21] In this method, we (1) exploited the advantages of a simple ionic liquid, butyl methylimidazolium chloride ($BMIm^+Cl^-$), a green solvent,[22−25] to develop an innovative, simple, pollution-free method to dissolve not only CS but also other polysaccharides including CEL without using any acid or base, thereby avoiding any possible chemical or physical changes, and (2) used only naturally occurring biopolymers such as CEL as support materials to strengthen the structure and expand the utility while keeping the biodegradable, biocompatible, anti-infective, and drug-carrier properties of CS-based materials intact. Using this method, we have successfully synthesized composite materials containing CEL and CS with different compositions. As expected, the composite materials obtained were found to have the combined advantages of their components, namely, superior chemical stability and mechanical stability (from CEL) and excellent antimicrobial properties (from CS). The [CEL + CS] composite materials inhibit the growth of a wider range of bacteria than other CS-based materials prepared by conventional methods. Specifically, it was found that over a 24 h period the composite materials substantially inhibited the growth of bacteria such as methicillin-resistant *Staphylococcus aureus* (MRSA), vancomycin-resistant *Enterococcus* (VRE), *S. aureus*, and *E. coli*.[21]

The information presented is indeed provocative and clearly indicates that it is possible to use this simple, one-step process without any chemical modification to synthesize novel supramolecular composite materials from CEL, CS, and CDs. On the basis of results from our previous work on the [CEL + CS] composites,[21] it is expected that the [CEL and/or CS + CD] composite materials may possess all of the properties of their components, namely, mechanical strength (from CEL) and excellent adsorbent for toxins and pollutants (from CS), and selectively form inclusion complexes with substrates of different sizes and shapes (from CDs). Such considerations prompted us to initiate this study, which aims to hasten the breakthrough by using the method that we developed recently to synthesize novel supramolecular composite materials from CEL, CS, and CDs. Results of the synthesis, spectroscopic characterization, and applications of the composite materials for the removal of organic pollutants such as endocrine disruptors are reported herein.

2. EXPERIMENTAL SECTION

2.1. Chemicals. Cellulose (microcrystalline powder) and chitosan (MW ≈ 310−375 kDa) were purchased from Sigma-Aldrich (Milwaukee, WI) and used as received. [$BMIm^+Cl^-$] was synthesized from freshly vacuum distilled 1-methylimidazole and 1-chlorobutane (Alfa Aesar, Ward Hill, MA) using a procedure previously used in our laboratory.[21,26] 2-Chlorophenol (2-Cl-Ph), 3-chlorophenol (3-Cl-Ph), 4-chlorophenol (4-Cl-Ph), 3,4-dichlorophenol (3,4-di-Cl-Ph), 2,4,5-trichlorophenol (2,4,5-tri-Cl-Ph), and bisphenol A (BPA) were from Sigma-Aldrich (Milwaukee, WI). Heptakis(2,3,6-tri-*O*-acetyl)-*β*-cyclodextrin (*β*-TCD) (TCI America, Portland, OR), hexakis(2,3,6-tri-*O*-acetyl)-*α*-cyclodextrin (*α*-TCD), and octakis(2,3,6-tri-*O*-acetyl)-*γ*-cyclodextrin (*γ*-TCD) (Cyclodextrin-Shop, The Netherlands) were used as received. See Scheme 1 for structures of the compounds used in this study.

2.2. Instrumentation. Elemental analysis was carried out by Midwest Microlab, LLC (Indianapolis, IN). ^{1}H NMR spectra were taken on a VNMRS 400 spectrometer. Near-infrared (NIR) spectra were recorded on a home-built NIR spectrometer.[27] FT-IR spectra were recorded on a PerkinElmer 100 spectrometer at 2 cm^{-1} resolution with either KBr or a ZnSe single-reflection ATR accessory (Pike Miracle ATR). X-ray diffraction (XRD) measurements were made on a Rigaku MiniFlex II diffractometer utilizing Ni-filtered Cu K*α* radiation (1.54059 Å).[28] Scanning electron microscopy images of the surface and cross section of the composite materials were recorded under vacuum with an acceleration voltage of 3 kV using a Hitachi S4800 scanning electron microscope (SEM). Tensile strength measurements were made on an Instron 5500R tensile tester.

2.3. Preparation of [CEL + TCD] and [CS + TCD] Composite Films. [CEL + *α*-TCD, *β*-TCD, and *γ*-TCD] and [CS + *α*-TCD, *β*-TCD, and *γ*-TCD] composite materials were synthesized using a procedure similar to that previously developed in our laboratory for the synthesis of CEL, CS, and [CEL + CS].[21] Essentially, as shown in Scheme 2, an ionic liquid, [$BMIm^+Cl^-$], was used as a solvent to dissolve CEL, CS, *α*-TCD, *β*-TCD, and *γ*-TCD. Dissolution was performed at 100 °C under an Ar or N_2 atmosphere. All polysaccharides were added in portions of approximately 1 wt % of the ionic liquid. Succeeding portions were added only after the previous addition had completely dissolved until the desired concentration had been reached. For composite films, the components were dissolved one after the other, with CEL (or CS) being dissolved

dx.doi.org/10.1021/la3050016 | *Langmuir* 2013, 29, 5037−5049

Scheme 1. Structures of Compounds Used

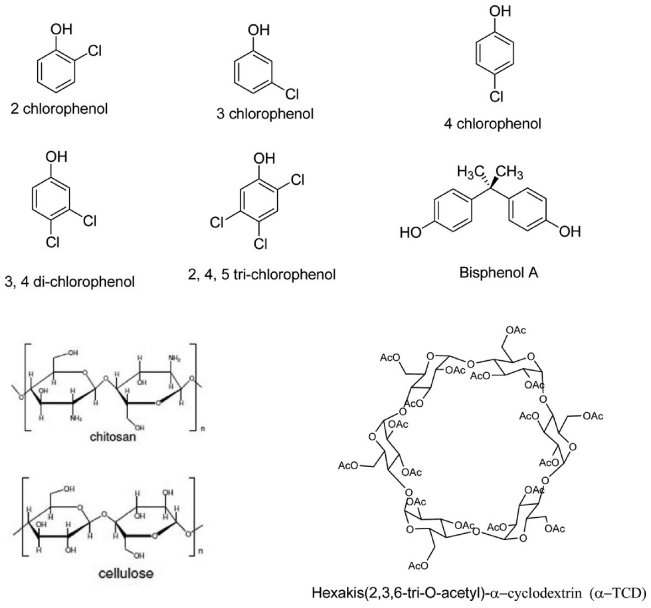

first and TCDs being dissolved last. When this procedure was used, solutions of CEL (containing up to 10% w/w IL), CS (up to 4% w/w), and composite solutions containing CEL (or CS) and α-TCD, β-TCD, or γ-TCD with various proportions were prepared in about 6–8 h.

Upon complete dissolution, the homogeneous solutions of the polysaccharides in [BMIm$^+$Cl$^-$] were cast on glass slides or Mylar sheets using an RDS stainless steel coating rod of the appropriate size (RDS Specialties, Webster, NY) to produce thin films with different compositions and concentrations of CEL (or CS) with α-TCD, β-TCD, or γ-TCD. If necessary, thicker composite materials can be obtained by casting the solutions onto PTFE molds of the desired thickness. They were then kept at room temperature for 24 h to allow the solutions to undergo gelation to yield GEL films. The [BMIm$^+$Cl$^-$] remaining in the film was then removed by washing the films in deionized water for about 3 days to yield WET films. During this period, the wash water was constantly replaced with fresh deionized water to maximize the removal of the ionic liquid. The [BMIm$^+$Cl$^-$] that was used was recovered from the washed aqueous solution by distillation. It was found that at least 88% of the [BMIm$^+$Cl$^-$] was recovered for reuse. The regenerated composite materials were lyophilized overnight to remove water, yielding dried porous composite films (DRY films).

2.4. Procedure Used to Measure the Kinetics of Adsorption. Two matching cuvettes were used for all adsorption measurements: one for the adsorption of the pollutant by the composite and the other as the blank (blank 1). A photograph of the two cells is shown in Figure SI-1 (Supporting Information). The samples (about 0.02 g of dry film of the composite material) were washed thoroughly in water prior to the adsorption experiments to further ensure that [BMIm$^+$Cl$^-$] was completely removed because the absorption of any residual IL may interfere with that of polychlorophenols or BPA. To wash the samples, the weighed composite materials were placed in a thin cell fabricated from PTFE whose windows were covered with two PTFE meshes. The meshes ensured free circulation of water through the material during the washing process. The PTFE mold containing the samples was placed in a 2 L beaker that was filled with deionized water and was stirred at room temperature for 24 h. During this time, the absorbance of washing water was monitored at 214 and 287 nm to determine the presence of any [BMIm$^+$Cl$^-$]. The water in the beaker was replaced with fresh deionized water every 4 h.

After 24 h, the composite material was taken out of the water and placed into the sample cuvette (cell on the right of the photograph shown in Figure SI-1). Both sample and blank cells were stirred using a small magnetic stir bar during the measurement. To prevent damage to the sample by the magnetic stir bar and to maximize the circulation of the solution during measurement, the samples were sandwiched between two PTFE meshes. Specifically, a piece of PTFE mesh was placed at the bottom of the spectrophotometric cell. The washed film sample was laid flat on top of the PTFE mesh. Another piece of PTFE mesh was placed on top of the sample, and finally the small magnetic stir bar was placed on top of the second mesh. The blank cell, shown on the left of the photograph in Figure SI-1, had the same contents as the sample cell but without the composite material. Exactly 2.70 mL of the 1.55×10^{-4} M aqueous solution of polychlorophenol or BPA was added to both the sample and blank cell. A second blank cell (blank 2) was also employed. Blank cell 2 had the same contents as the sample cell (i.e., PTFE mesh, composite film, PTFT mesh, and magnetic stir bar) but without the pollutant. Any adsorption of the pollutants by the

Scheme 2. Procedure Used to Prepare the Cellulose–Chitosan–TCD Composite Materials

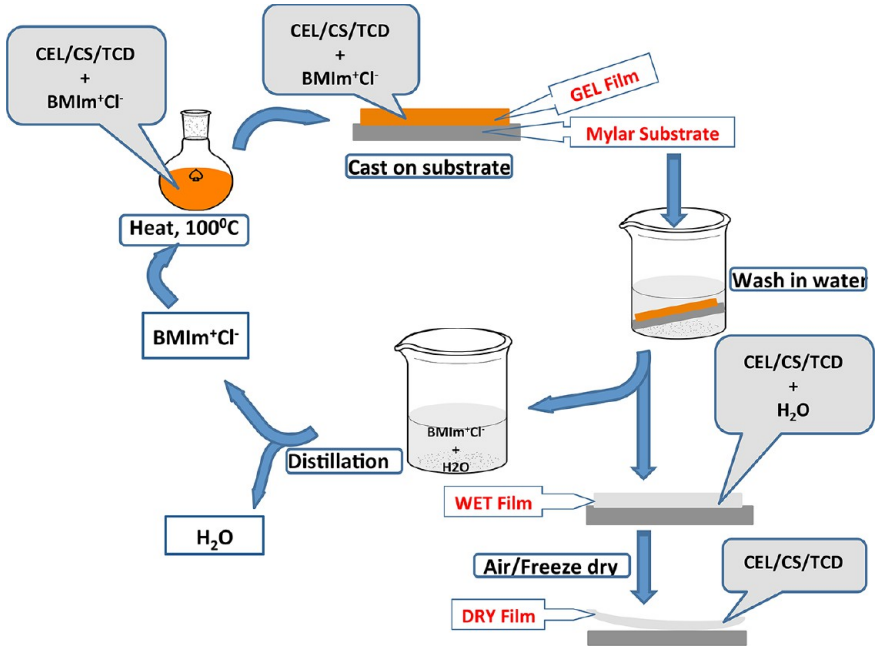

dx.doi.org/10.1021/la3050016 | Langmuir 2013, 29, 5037–5049

cell contents (PTFE mesh, magnetic stir bar) and not by the composite materials was corrected by the signal of blank 1. Blank 2 provided information on any possible interference of absorption of pollutants by the leakage of residual IL from the composite film. Measurements were carried out on a Perkin-Elmer Lambda 35 UV/vis spectrometer set to the appropriate wavelength for each pollutant (i.e., 274 nm for 2- and 3-chlorophenol, 280 nm for 4-chlorophenol, 282 and 289 nm for 3,4-dichloro- and 2,4,5-trichlorophenol, respectively, and 276 nm for bisphenol A). Measurements were taken at 10 min intervals during the first 2 h and at 20 min intervals after 2 h. After each measurement, the cell was returned to the magnetic stirrer for continuous stirring. Reported values were the difference between the sample signals and those of blanks 1 and 2. However, it was found that signals measured by both blank cells were negligible within experimental error.

2.5. Procedure Used to Measure Equilibrium Sorption Isotherms. Batch sorption experiments were carried out in 50 mL stoppered vials containing 10 mL of the pollutant solution of known initial concentration. A weighed amount (0.1g) of the composite material was added to the solution. The samples were agitated at 250 rpm in a shaking water bath at 25 °C for 72 h. The residual amount of pollutant in each flask was analyzed by UV/vis spectrophotometry. The amount of pollutant adsorbed onto the composite material was calculated using the following mass balance equation

$$q_e = \frac{(C_i - C_e)V}{m} \quad (1)$$

where q_e (mg/g) is the equilibrium sorption capacity and C_i and C_e (mg/L) are the initial and final pollutant concentrations, respectively. V (L) is the volume of the solution, and m (g) is the weight of the composite film material.

Detailed information on the analysis of kinetic data and equilibrium sorption isotherms can be found in the Supporting Information.

3. RESULTS AND DISCUSSION

3.1. Synthesis and Characterization of CEL/CS + α-TCD, β-TCD, and γ-TCD Composites; Materials Used. The CS used in this study was specified by the manufacturer (Sigma-Aldrich) as having a degree of deacetylation (DA) value of 75%. As will be described below, because unique properties of CS including its ability to adsorb pollutants are due to its amino groups, experiments were performed to determine its DA value. Two different methods, FT-IR and ^{1}H NMR, were employed for the determination.[30−35] For the FT-IR method, the spectra were taken at 2 cm^{-1} resolution. The CS sample was vacuum-dried at 50 °C for 2 days. A small amount of the dried sample was then ground into KBr and pressed into a pellet for FT-IR measurements. Four KBr pellets were prepared, and their spectra were recorded. The degree of deacetylation (DA) was calculated from the four spectra, and the average value is reported together with the standard deviation. The DA value was calculated on the basis of the following equation[30,31]

$$\mathrm{DA}(\%) = 100 - \left[\frac{\left(\frac{A_{1655}}{A_{3450}}\right)100}{1.33}\right] \quad (2)$$

where A_{1655} and A_{3450} are the absorbance at 1655 cm^{-1} of the amide C═O and the absorbance at 3450 cm^{-1} of the OH band, respectively. The factor 1.33 denotes the value of the ratio of A_{1655}/A_{3450} for fully N-acetylated chitosan. A DA% value of 84 ± 2 was found using this method.

For the ^{1}H NMR determination, the spectra were taken at 70 °C. About 5 mg of the chitosan sample that was previously vacuum-dried at 50 °C for 2 days was dissolved in 0.5 mL of 2 wt % DCl/D_2O solution at 70 °C. The degree of deacetylation (DA) was evaluated from the following equation using the integral intensity, I_{CH_3}, of the CH_3 residue of *N*-acetyl and the sum of the integral intensities, I_{H2-H6}, of protons 2−6 of the chitosan residue:[35]

$$\mathrm{DA}(\%) = \left[1 - \left(\frac{\frac{1}{3}I_{CH_3}}{\frac{1}{6}I_{H2-H6}}\right)\right]100 \quad (3)$$

A DA value of 78% was found using this method.

It has been reported that chitosan samples may contain some protein impurities. Accordingly, experiments were carried out to determine any possible protein impurities in the CS sample used in this study. The percentage of proteins impurity (%*P*) can be calculated from the following equation[36−38]

$$\%P = (\%\mathrm{N} - \mathrm{N_T})6.25 \quad (4)$$

where 6.25 corresponds to the theoretical percentage of nitrogen in proteins, %N represents the percentage of nitrogen measured by elemental analysis, and N_T represents the theoretical nitrogen content of the chitosan sample. It was calculated on the basis of the degree of deacetylation (DA) of chitosan and the percentage of nitrogen for fully acetylated chitin and fully deacetylated chitosan (6.89 and 8.69),[36−38] respectively. Using DA values of 84% (from FT-IR) and 78% (from NMR), the percentages of protein impurities in the CS sample were found to be 1.89 and 1.24%, respectively. When errors associated with elemental analysis and with the determination of DA values by the FT-IR and NMR methods are taken into account, it can be assumed that these two %*P* values are the same within experimental error.

As described in the Experimental Section, [BMIm$^+$Cl$^-$] was used as the sole solvent to dissolve CEL, CS, and TCD to prepare the [CEL + TCD] and [CS + TCD] composite materials. It is noteworthy to add that [BMIm$^+$Cl$^-$] is not the only IL that can dissolve the polysaccharides. Other ILs including ethylmethylimidazolium acetate (EMIm$^+$Ac$^-$), BMIm$^+$Ac$^-$, and allylmethylimidazolium chloride (AMIm$^+$Cl$^-$) are also known to dissolve the polysaccharides as well. [BMIm$^+$Cl$^-$] was selected because compared to these ILs it can dissolve relatively higher concentrations of polysaccharides. For example, the solubility of CEL in [BMIm$^+$Cl$^-$], [AMIm$^+$Cl$^-$], [BMIm$^+$Ac$^-$], and [EMIm$^+$Ac$^-$] was reported to be 20, 15, 12 and 8%, respectively. Furthermore, [BMIm$^+$Cl$^-$] is cheaper than these ILs because it can easily be synthesized in a one-step process from relatively inexpensive reagents (1-methylimidazole and 1-chlorobutane) whereas other ILs are more expensive because they require more expensive reagents (silver acetate) and a two-step synthesis process.[29,39−43]

Because [BMIm$^+$Cl$^-$] is totally miscible with water, it was removed from the gel films of the composites by washing the films with water. The wash water was repeatedly replaced with fresh water until it was confirmed that there were no ILs in the wash water (by monitoring the UV absorption of the IL at 214 and 287 nm). The IL used was recovered by distilling the washed aqueous solution (the IL remained because it is not volatile). The recovered [BMIm$^+$Cl$^-$] was dried under vacuum at 70 °C overnight before reuse. It was found that at least 88% of [BMIm$^+$Cl$^-$] was recovered for reuse. As such, the method developed here is recyclable because [BMIm$^+$Cl$^-$] is the only

dx.doi.org/10.1021/la3050016 | Langmuir 2013, 29, 5037−5049

solvent used in the preparation and the majority of it was recovered for reuse.

The dissolution of the polysaccharides, for example, CS and TCD, in the [BMIm$^+$Cl$^-$] ionic liquid and their regeneration in the composite materials was followed and studied by powder X-ray diffraction (XRD). Figure 1 shows the XRD spectra of the

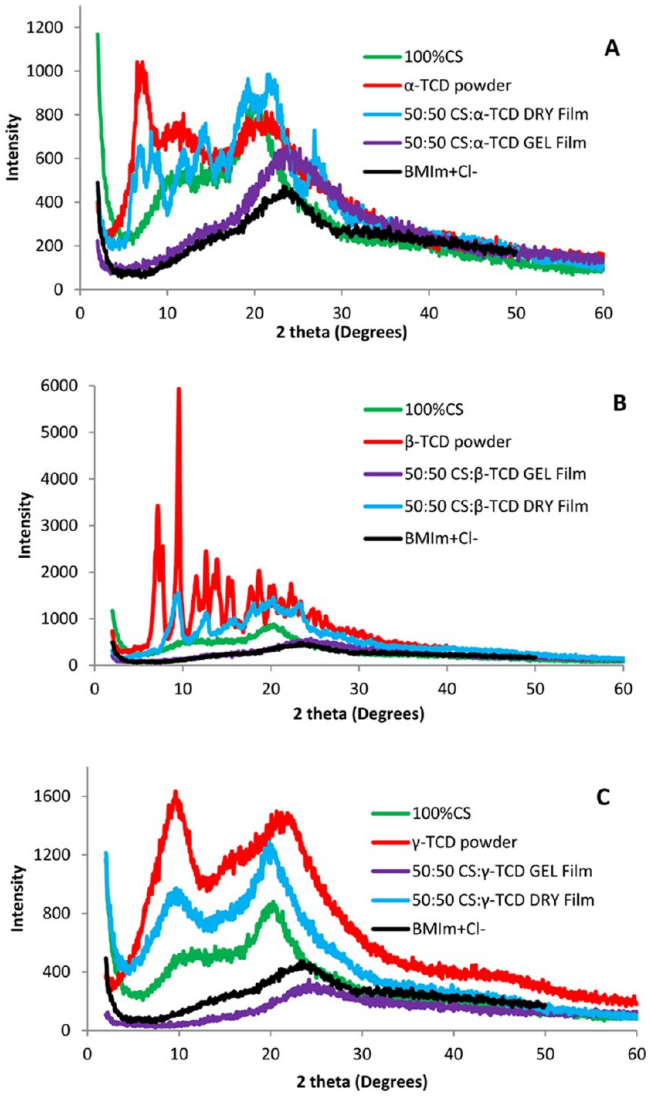

Figure 1. X-ray powder diffraction spectra of [BMIm$^+$Cl$^-$]; CS powder; α-TCD, β-TCD, and γ-TCD powder; and (A) [CS + α-TCD] , (B) [CS + β-TCD], and (C) [CS + γ-TCD] composite materials at different stages of synthesis.

[CS + α-TCD], [CS + β-TCD], and [CS + γ-TCD] composites at various stages of preparation. The difference among XRD spectra of the α-, β-, and γ-TCD materials (red curves in Figure 1A–C, respectively) seems to indicate that these starting cyclodextrin materials have different structural morphologies. Although the XRD spectrum of the β-TCD powder is consistent with a highly crystalline structure, the XRD spectra of α-TCD and γ-TCD seem to suggest that these CDs have an amorphous structure.[2] The XRD spectra of [BMIm$^+$Cl$^-$] (black curves) and the gel films (purple curves) were obtained to determine the dissolution of the CS and TCDs in the ionic liquid. As illustrated, the XRD spectra of the gel films are similar to that of [BMIm$^+$Cl$^-$] and do not exhibit any of the CS or TCD diffraction peaks. The absence of the XRD peaks of CS and TCDs and the similarity between the spectra of the gel films to that of the [BMIm$^+$Cl$^-$] clearly indicate that [BMIm$^+$Cl$^-$] completely dissolved CS and TCDs. The XRD spectra of the regenerated composite films (dry films) are also shown as blue curves in Figure 1. As expected, the XRD spectra of the 50:50 CS/α-TCD, 50:50 CS/β-TCD, and 50:50 CS/γ-TCD regenerated composite films exhibit XRD peaks that can be attributed to those of α-TCD, β-TCD, and γ-TCD, respectively.

FT-IR and NIR spectroscopy was used to characterize the chemical composition of the resultant composite films. The FT-IR and NIR spectra of the α-TCD powder, 100% CS, and [CS + α-TCD] composite materials are shown in Figure 2A,B, respectively. (Those corresponding to β-TCD and γ-TCD are shown in Figures SI-2A,B and SI-3A,B in the Supporting Information.) As illustrated, the FT-IR spectrum of a 100% CS dried film displays characteristic CS bands around 3400 cm^{-1} (O–H stretching vibrations), 3250–3350 cm^{-1} (symmetric and asymmetric N–H stretching), 2850–2900 cm^{-1} (C–H stretching), 1657 cm^{-1} (C═O, amide 1), 1595 cm^{-1} (N–H deformation), 1380 cm^{-1} (CH_3 symmetrical deformation), 1319 cm^{-1} (C–N stretching, amide III), and 890–1150 cm^{-1} (ether bonding).[21,44−47] For reference, the FT-IR spectrum of the α-TCD starting material is also shown as a red curve in Figure 2A (and those β- and γ-TCD powders are in Figure SI-1A,B, respectively). The spectrum of the α-TCD powder in Figure 2A and that of the β- and γ-TCD powders in Figures SI-2A,B are very similar to one another, which is as expected because these three compounds differ only in the number of glucose moieties making up the ring. The dominant absorption bands of these spectra are those due to the C═O stretching vibration at ∼1746 cm^{-1}; medium and weak bands at ∼1372 and 1434 cm^{-1} can be attributed to the symmetric and asymmetric deformations of the CH_3 group of acetates, the C–O asymmetric stretching vibration of acetates at ∼1216 cm^{-1}, and the asymmetric stretching vibration of the O–CH_2–C groups for acetates.[21,47,48] Also included as a blue curve is the FT-IR spectrum of the 50:50 CS/α-TCD composite film. In addition to bands due to CS, the composite material also exhibits, as expected, all bands that are due to α-TCD as described above.

Results from NIR measurements further confirm the successful incorporation of the TCDs into CS (Figures 2B and SI-3) and CEL (Figure SI-4 in the Supporting Information). The 100% CS film exhibits NIR absorption bands at around 1492, 1938, and 2104 nm (Figure 2B), which can be assigned to the overtone and combination transitions of the –OH group.[21,28,46,48] In addition, CS also exhibits bands at ∼1548 and 2028 nm that are due to the –NH groups.[49]

Similar to FT-IR, the NIR spectra of α-, β-, and γ-TCD are also very similar. The major bands for these are around 1415 nm (first overtone of the methyl –CH group), 1680 and 1720 nm (first overtone of the –CH group), and 1908 and 2135 nm (–C═O, acetyl group).[50] As shown in Figure 2B (and Figure SI-3A,B), the NIR spectra of [CS + α-TCD], [CS + β-TCD], and [CS + γ-TCD] composite materials contain bands due to both CS and TCDs.

Similarly, FT-IR and NIR results also confirm that α-TCD, β-TCD, and γ-TCD were successfully incorporated into CEL. For clarity, the FT-IR and NIR spectra of only the β-TCD powder and 50:50 CEL/β-TCD together with the 100% CEL film are shown in Figure SI-4A,B, respectively. The 100% CEL film

dx.doi.org/10.1021/la3050016 | Langmuir 2013, 29, 5037–5049

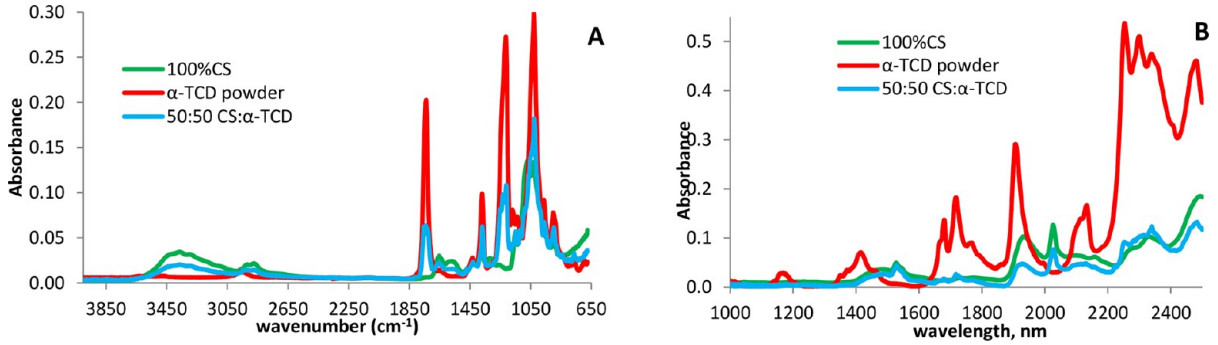

Figure 2. (A) FTIR and (B) NIR spectra of 100% CS, α-TCD, and 50:50 CS/α-TCD composite material.

(green curve in Figure SI-4A) exhibits three pronounced bands at around 3400, 2850−2900, and 890−1150 cm^{-1}. These bands can be tentatively assigned to stretching vibrations of the O−H, C−H, and −O− groups, respectively.[44] Similar to the CS composite materials, FT-IR and NIR spectra of the [CEL + β-TCD] composite material (as well as [CEL + α-TCD] and [CEL + γ-TCD] composites, spectra not shown) also exhibit bands due to both TCDs and CEL.

An analysis of the composite materials by SEM reveals some interesting features about the microstructure of the materials. Shown in Figure 3 are surface (images on left column) and cross-section images (images on right column) of regenerated one-component 100% CEL and 100% CS films (first and second rows) and 50:50 [CEL + γ-TCD], [CEL + β-TCD], [CS + γ-TCD], and [CS + β-TCD] (rows 3−6). As expected, both surface and cross section images clearly indicate that one-component CEL and CS are homogeneous. Chemically, the only difference between CS and CEL is amino in the former. However, their structures, as recorded by the SEM, are substantially different. Specifically, whereas CS exhibits a rather smooth structure, CEL seems to arrange itself into a fibrous structure with fibers having a diameter of about ∼0.5−1.0 μm. Interestingly, the structure of a 50:50 composite between CS and γ-TCD (images on row 5) seems to be very much different from that of 50:50 [CS + β-TCD] (images on row 6). SEM images of the latter seem to indicate that it has a rather smooth structure that is different from the rather fibrous structure of the 50:50 [CS + γ-TCD] composite. Similarly, the microstructure of 50:50 [CEL + γ-TCD] (row 3) is also different from that of [CEL + β-TCD]. It is known that β-CD, being relatively small, has a rather rigid structure whereas the large γ-CD has a more flexible structure. Also, γ-CD is very soluble in water (23.2 g/100 mL) whereas β-CD can hardly dissolve in water (1.85 g/100 mL). It is possible that because of these differences, when β-TCD forms a composite with either CS or CEL, it will adopt a microstructure that is much different from that of a composite between γ-TCD with either CEL or CS.

As described above, the mechanical and rheological strength of CDs is so poor that they practically cannot be fabricated into films for applications. Measurements were made to determine the tensile strength of [CEL + TCDs] and [CS + TCDs] composite films with different CEL and CS concentrations to determine if adding CEL or CS would provide the composite material with adequate mechanical strength for practical applications. The results obtained, shown in Figure 4, clearly indicate that adding either CEL or CS to the composite materials substantially increases their tensile strength. For example, up to a 2-fold (or 6-fold) increase in tensile strength can be achieved by increasing the concentration of CEL in the

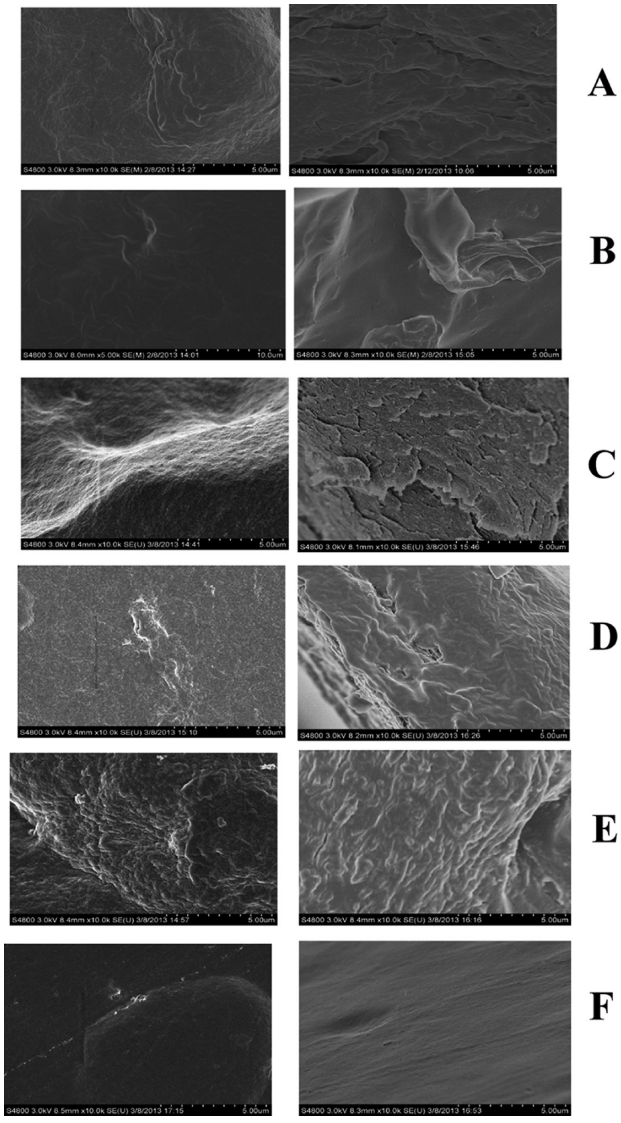

Figure 3. SEM images of the surface (images on left column) and cross section (images on right column) of (A) 100% CEL, (B) 100% CS, (C) 50:50 CEL/γ-TCD, (D) 50:50 CEL/β-TCD, (E) 50:50 CS/γ-TCD, and (F) 50:50 CS/β-TCD.

[CEL + γ-TCD] composite (or CS in the [CS + γTCD] composite) from 50 to 75%. Also, the tensile strength of the [CEL + γ-TCDs] composite is relatively higher than that of the corresponding [CS + γ-TCDs] composite. This is hardly surprising considering the fact that the mechanical and

dx.doi.org/10.1021/la3050016 | *Langmuir* 2013, 29, 5037−5049

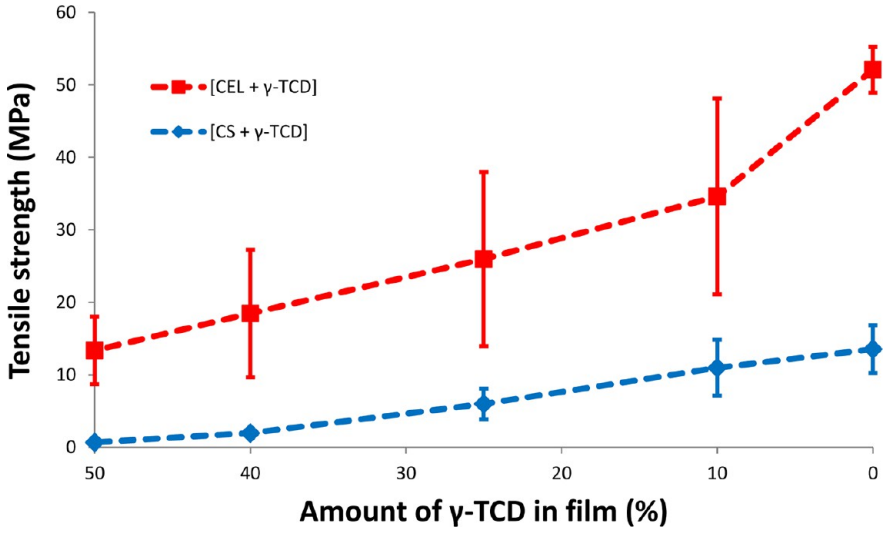

Figure 4. Plot of tensile strength as a function of γ-TCD concentration in [CEL + γ-TCD] composites (red curve) and [CS + γ-TCD] composites (blue curve).

rheological strength of CEL is relatively higher than that of CS. It is thus evidently clear that the [CEL + TCD] and [CS + TCD] composite materials have overcome the major hurdle currently imposed on the utilization of the materials, namely, they have the required mechanical strength for practical applications.

Taken together, the XRD, FT-IR, NIR, and SEM results presented clearly indicate that all novel polysaccharide composite materials containing CEL, CS, α-TCD, β-TCD, and γ-TCD were successfully synthesized by the use of [$BMIm^+Cl^-$], an ionic liquid, as the sole solvent. Because the majority (at least 88%) of [$BMIm^+Cl^-$] used was recovered for reuse, the method is recyclable. As anticipated, adding CEL (or CS) to the composites substantially increases the mechanical strength of the composites. It is expected that the composites may also retain the properties of CS and TCDs,; namely, they would be good adsorbents for pollutants (from CS) and selectively form inclusion complexes with substrates of different sizes and shapes (from TCDs). The initial evaluation of their ability to adsorb various endocrine disruptors selectively, including polychlrophenols and bisphenol A, is described in the following section.

3.2. Adsorption of Endocrine Disruptors (2-, 3-, and 4-Chlorophenol, 3,4-Dichlorophenol, 2,4,5-Trichlorophenol, and Bisphenol A). *3.2.1. Adsorption Kinetics.* Experiments were designed to determine (1) if CEL, CS, [CEL + TCD], and [CS + TCD] composite materials can adsorb chlorophenols and bisphenol A; (2) if they can, the rate constants, adsorbed amounts at equilibrium (q_e), and mechanism of adsorption processes; (3) the composite material that gives the highest adsorption; and (4) if TCDs can provide any selectivity on adsorption of analytes with different sizes and shapes. These were accomplished by initially fitting the kinetic data to both pseudo-first-order and pseudo-second-order models. The appropriate reaction order for the adsorption processes was determined on the basis of the correlation coefficients (R^2) and the model selection criteria (MSC) values. Rate constants and q_e values were then obtained from the kinetic results.[51,52] The subsequent fitting of data to the intraparticle diffusion model together with the results of adsorption isotherm measurements yielded additional insight into the adsorption process.

The pseudo-first-order and pseudo-second-order kinetic models were used to obtain the rate constants and equilibrium adsorption capacity of 100% CEL, 100% CS, 50:50 CS:/β-TCD, and 50:50 CEL/β-TCD composite materials for different analytes including chlorophenols and bisphenol A. Results obtained by the pseudo-first-order and pseudo-second-order fitting of adsorption of all analytes by 100% CEL, 100% CS, 50:50 CS/β-TCD, and 50:50 CEL/β-TCD are listed in Tables SI-1−4 (of the Supporting Information). In all cases, the R^2 and MSC values are higher for the pseudo-second-order kinetic model than those corresponding to the pseudo-first-order kinetic model. In addition, the theoretical and experimental equilibrium adsorption capacities, q_e, obtained for the pseudo-first-order kinetic model varied widely for the different analytes. The results seem to suggest that the adsorption of various chlorophenols and BPA onto 100% CEL, 100% CS, 50:50 CS/β-TCD, and 50:50 CEL,β-TCD composite materials is best described by the pseudo-second-order kinetic model. Good correlation of the system provided by the pseudo-second-order kinetic model suggests that chemical sorption involving valence forces through the sharing or exchange of electrons between adsorbents and analytes might be significant.[52]

Additional information on mechanism of adsorption can be gained by analyzing data using the intraparticle diffusion model as described in the Supporting Information. Shown in Figure 5 are representative intraparticle pore diffusion plots (q_t vs $t^{1/2}$) for three of the analytes studied: 3,4-di-Cl-Ph, 2,4,5-tri-Cl-Ph, and BPA adsorbed on 50:50 CEL/β-TCD and 50:50 CS/β-TCD composites. As illustrated, plots of q_t versus $t^{1/2}$ are not linear but rather are nonlinear and can be fitted to two linear segments for all analytes on both composites with the exception that data for 2,4,5-tri-Cl-Ph on 50:50 CS/β-TCD may possibly be fitted to a linear regression with $R^2 = 0.9819$. According to this model, the first sharper linear region can be assigned to the instantaneous adsorption or external surface adsorption, and the second region may be due to the gradual adsorption stage where intraparticle diffusion is rate-limiting.[51,53] These results seem to imply that the intraparticle diffusion is not the sole

dx.doi.org/10.1021/la3050016 | *Langmuir* 2013, 29, 5037−5049

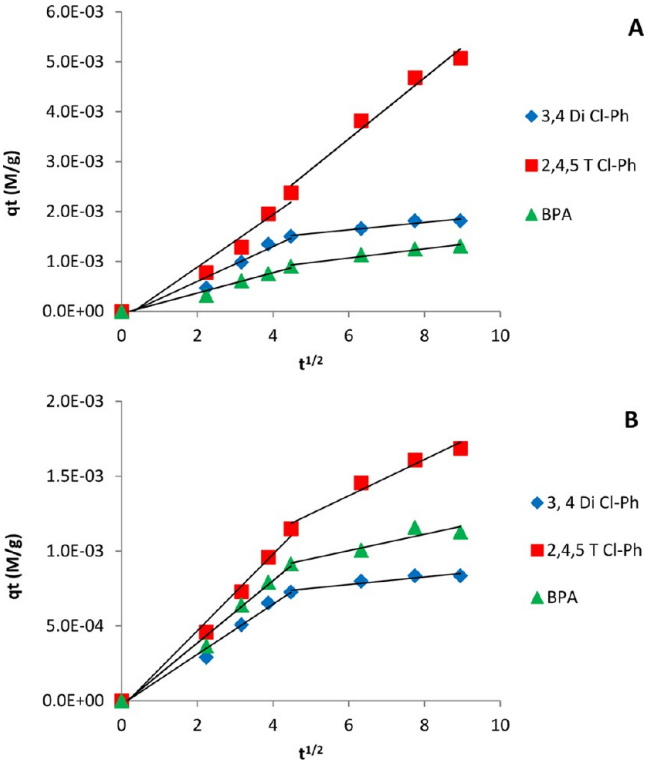

Figure 5. Intraparticle pore diffusion model plots for (A) 50:50 CS/β-TCD and (B) 50:50 CEL/β-TCD.

rate-controlling step but other mechanisms may also contribute to the adsorption process.

Results obtained from the pseudo-second-order kinetics in terms of the equilibrium sorption capacity (q_e) and rate constant (k_2) were then used to evaluate the sorption performance of the composite materials. Table 1 lists q_e and k_2 values for five different chlorophenols and BPA on 100% CEL, 50:50 CEL/β-TCD, 100% CS, and 50:50 CS/β-TCD, respectively. For clarity of presentation and discussion, data from the tables were used to construct three plots for three pairs of composites: 100% CEL and 100% CS (Figure 6A), 100% CEL and 50:50 CEL/β-TCD (Figure 6B), and 100% CS and 50:50 CS/β-TCD (Figure 6C). Figure 6D plots results obtained for all analytes by all composite materials.

It is evident from Figure 6A that, for all analytes, equilibrium sorption capacities for the 100% CS material are much higher than those corresponding to the 100% CEL material (e.g., for 2,4,5-tri-Cl-Ph, the 100% CS material exhibits up to 6-fold more equilibrium sorption capacity than the 100% CEL material). Even for BPA, where the difference between CEL and CS materials is smallest, the CS material still has a q_e value that is twice that of the CEL material. This is as expected because CEL is known to be inert whereas CS is reported to be an effective adsorbent for various pollutants.

Additional experiments were then performed to confirm these results. Specifically, six different [CEL + CS] composite materials with different CEL and CS compositions were synthesized, and their adsorption of 2,4,5-trichlorophenol was measured. The results obtained in terms of q_e and k_2 values, plotted as a function of CS concentration in the composites, are shown in Figure 7A. It is evident that adding CS to CEL resulted in an improved uptake of 2,4,5-trichlorophenol. For example, the q_e value was increased by 5-folds when 50% CS

Table 1. Comparison of Pseudo-Second-Order Kinetic Parameters for 100% CEL, 100% CS, 50:50 CEL/β-TCD, and 50:50 CS/β-TCD Composite Materials

	100% CEL				100% CS				50:50 CEL:β-TCD				50:50 CS:β-TCD			
analyte	q_e(M/g)	k_2 (M^{-1} min^{-1})	R^2	MSC	q_e(M/g)	k_2 (M^{-1} min^{-1})	R^2	MSC	q_e(M/g)	k_2 (M^{-1} min^{-1})	R^2	MSC	q_e(M/g)	k_2 (M^{-1} min^{-1})	R^2	MSC
2-ClPh	3.93×10^{-4}	702.3	0.9871	3.95	1.32×10^{-3}	385.9	0.9998	8.02	1.30×10^{-3}	100.2	0.9975	5.57	7.58×10^{-4}	268.4	0.9967	5.32
3-ClPh	3.20×10^{-4}	293.8	0.9822	3.72	1.68×10^{-3}	133.5	0.9960	5.21	9.87×10^{-4}	77.9	0.9964	5.33	1.25×10^{-3}	118.6	0.9934	4.71
4-ClPh	5.81×10^{-4}	2054.2	0.9999	9.13	1.66×10^{-3}	214.6	0.9996	7.52	1.41×10^{-3}	58.0	0.9993	6.93	8.99×10^{-4}	313.1	0.9957	5.11
3,4 Di-ClPh	8.19×10^{-4}	315.6	0.9996	7.47	2.27×10^{-3}	169.8	0.9999	8.72	9.12×10^{-4}	160.6	0.9992	6.84	1.99×10^{-3}	57.1	0.9978	5.77
2,4,5 Tri-ClPh	1.95×10^{-3}	25.4	0.9967	5.32	1.20×10^{-2}	2.1	0.9991	6.60	2.00×10^{-3}	33.2	0.9995	7.26	8.84×10^{-3}	2.1	0.9996	7.41
BPA	8.05×10^{-4}	78.9	0.9911	4.39	1.80×10^{-3}	168.3	0.9995	7.24	1.34×10^{-3}	65.5	0.9987	6.28	1.59×10^{-3}	37.6	0.9994	7.11

dx.doi.org/10.1021/la3050016 | *Langmuir* 2013, 29, 5037−5049

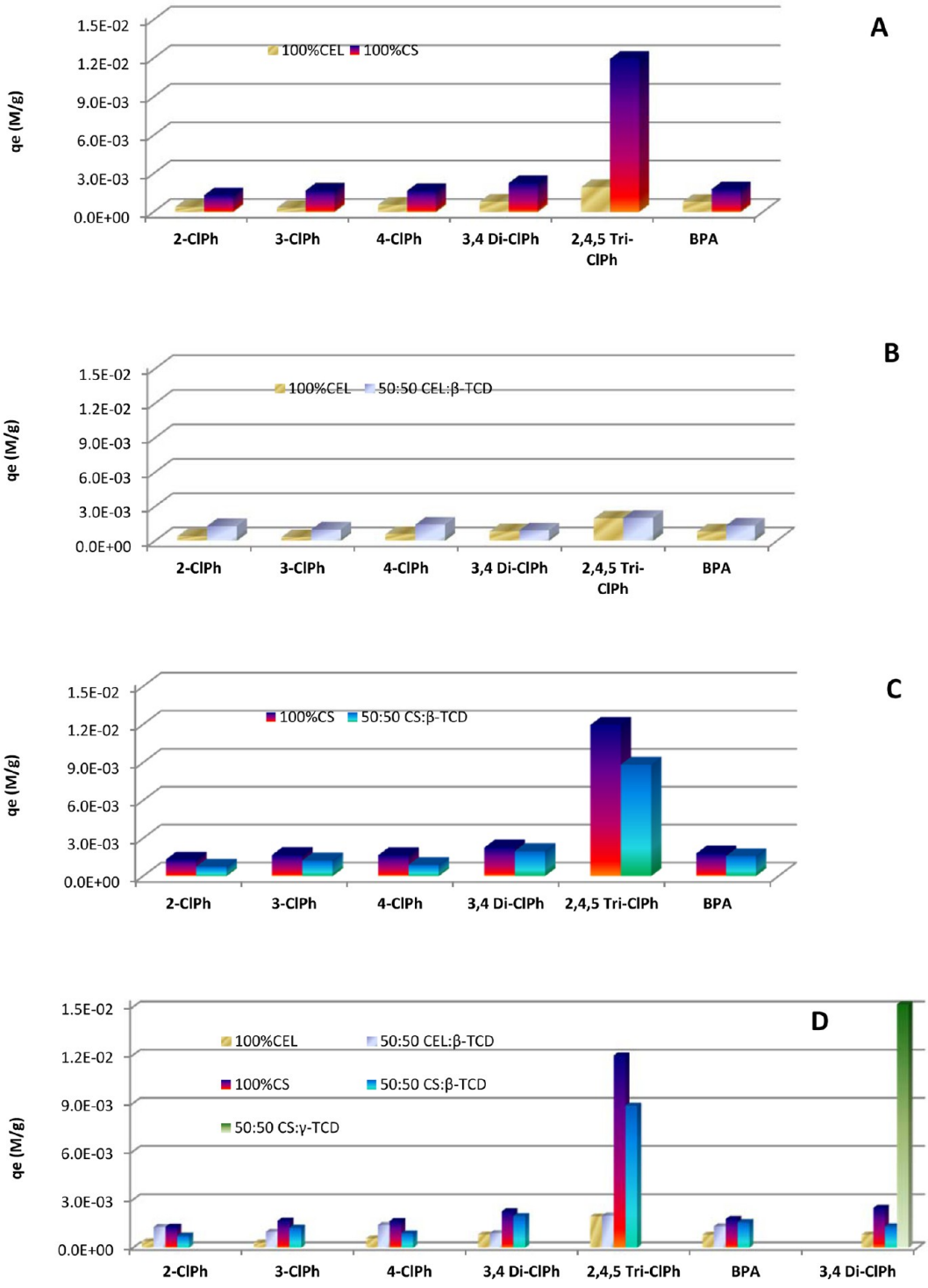

Figure 6. Plot of equilibrium sorption capacity (q_e) of all analytes by (A) 100% CEL and 100% CS, (B) 100% CEL and 50:50 CEL/β-TCD, (C) 100% CS and 50:50 CEL/β-TCD, and (D) all four composites.

was added to CEL, and the equilibrium sorption capacity seems to be proportional to the concentration of CS in the composite. These results clearly indicate that CS is responsible for the adsorption of the endocrine disruptors and that the sorption capacity of a composite toward endocrine disruptors can be set to any value by judiciously adjusting the concentration of CS in the composite.

When added to CEL, β-TCD seems to exert a much different effect on the equilibrium sorption capacity than does CS. As illustrated in Figure 6B, a substantial enhancement in q_e values was observed when 50% β-TCD was added to CEL, but the enhancement was not observed for all analyte (as seen for CS) but only for four analytes (i.e., about a 3-fold enhancement for 2- and 3-chlorophenol and about a 2-fold enhancement for 4-chlorophenol and bisphenol A). Within experimental error, no observable enhancement was observed for 3,4-dichlorophenol and 2,4,5-trichlorophenol when 50% β-TCD was added to CEL. A variety of reasons might account for the lack of

dx.doi.org/10.1021/la3050016 | *Langmuir* 2013, 29, 5037−5049

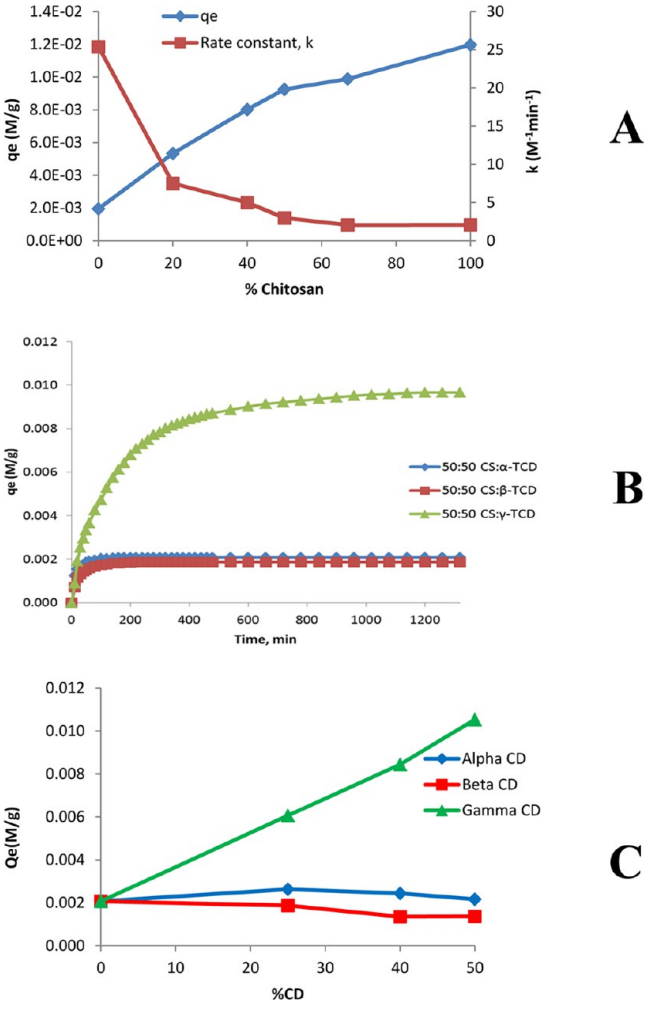

Figure 7. Plot of (A) q_e and k for the adsorption of 2,4,5-trichlorophenol as a function of CS concentration in [CEL + CS] composite materials. (B) Sorption profiles of 50:50 CS/α-TCD, 50:50 CS/β-TCD, and 50:50 γ-TCD CS composites for 3,4-di-Cl-Ph. (C) Equilibrium sorption capacity for 3,4-dichlorophenol by CS + TCD composite materials as a function of α-TCD, β-TCD, and γ-TCD concentrations in the composites.

enhancement for 3,4-dichloro and 2,4,5-trichlorophenol, but the most likely one is probably due to the bulky dichloro and trichloro groups on these compounds, which sterically hinder their ability to form inclusion complexes with β-TCD.

To investigate further the different effects of CS and β-TCD on the adsorption process, adsorption results by 100% CS and 50:50 CS/β-TCD for all analytes were plotted in Figure 6C. Compared to β-TCD, CS has relatively higher q_e values for all analytes, including 3,4-dichloro- and 2,4,5-trichlorophenol. The latter two compounds, as described above, may not be able to be included in the cavity of β-TCD because of their bulky groups. The results seem to indicate that CS may adsorb the analytes by a mechanism that is different from that of β-TCD; namely, surface adsorption appears to be the main and only adsorption mechanism for CS whereas inclusion complex formation seems to be the main adsorption process for β-TCD, with surface adsorption being the secondary mechanism. It is expected that whereas the efficiency for surface adsorption by CS is relatively higher than that of inclusion complex formation it may not provide any selectivity with respect to the size and shape of the host or guest compounds. To investigate this possibility, the adsorption of 3,4-dichlorophenol by 50:50 CS/γ-TCD as well as by 100% CEL, 100% CS, 50:50 CEL/β-TCD, and 50:50 CS/β-TCD was measured and the results are presented as the last group on the far right in Figure 6D. As expected, the results obtained further confirm the proposed mechanism. Specifically, 3,4-dichlorophenol, as described in the previous section, because of its bulky dichloro group, cannot form inclusion complexes with β-TCD. Therefore, it was adsorbed by CS as well as by β-TCD mainly through surface adsorption. Conversely, γ-TCD with its cavity being about 58% larger than that of β-TCD, can well accommodate 3,4-dichlorophenol in its cavity through inclusion complex formation that leads to a substantial enhancement in the adsorption capacity for 50:50 CS/γ-TCD as compared to that of other composites.

Additional evidence to confirm inclusion complex formation and size selectivity provided by TCD is shown in Figure 7B, which plots the sorption profiles for 3,4-dichlorophenol by 50:50 CS/α-TCD, 50:50 CS/β-TCD, and 50:50 CS/γ-TCD. As expected, because the cavities of α-TCD and β-TCD are too small to accommodate 3,4-dichlorophenol, the latter can be adsorbed only onto 50:50 CS/α-TCD and 50:50 CS/β-TCD by surface adsorption, which led to small, similar adsorption curves for both composite materials. Conversely, 50:50 CS/γ-TCD with its larger γ-TCD can readily form inclusion complexes with 3,4-dichlorophenol and, as a consequence, can adsorb much more analyte (i.e., a substantially higher sorption profile).

Plots of the equilibrium sorption capacity (q_e) for 3,4-dichlorophenol by CS + α-TCD, CS + β-TCD, and CS + γ-TCD as a function of α-, β-, and γ-TCD concentrations in the composites are shown in Figure 7C. Again, because 50:50 CS/α-TCD and 50:50 CS/β-TCD cannot form inclusion complexes with 3,4-dichlorophenol, their q_e values remain the same regardless of the concentrations of α- and β-TCD in the composite materials. Not only is the q_e profile of the CS + γ-TCD material different and much higher than those for CS + α-TCD and CS + β-TCD but also the q_e value is proportional to the concentration of γ-TCD in the composite material. For example, adding 50% γ-TCD to the CS material led to up to a 5-fold increase in the q_e value. This is probably due to the fact that because γ-TCD can readily form inclusion complexes with 3,4 dichlorophenol, increasing the concentration of γ-TCD in the [CS + γ-TCD] material resulted in a higher concentration of inclusion complexes and hence a higher q_e value.

3.2.2. Adsorption Isotherms. To gain insight into the adsorption process, an investigation was then carried out to determine the adsorption isotherm for the adsorption of 3,4-dichlorophenol by 100% CS and 50:50 CS/γ-TCD. These two composites were selected because the kinetic results presented above indicate that they adsorb 3,4-dichlorophenol by two distinct different mechanisms: surface adsorption and inclusion complex formation. The experimental results were fitted to three different models: the Langmuir isotherm,[54] Freundlich isotherm,[55] and Dubinin−Radushkevich (D−R) isotherm.[56,57] (See the Supporting Information for a detailed description of these three models.) The fitting of the experimental values to these three models is shown in Figure 8. The parameters obtained from fits to these models are listed in Table 2. As listed, the experimental values fit relatively well to the theoretical models. For example, R^2 values for the fit of 100% CS and 50:50 CS:/γ-TCD composites to the Langmuir, the Freundlich, and the D−R models were found to be 0.977 and

dx.doi.org/10.1021/la3050016 | Langmuir 2013, 29, 5037−5049

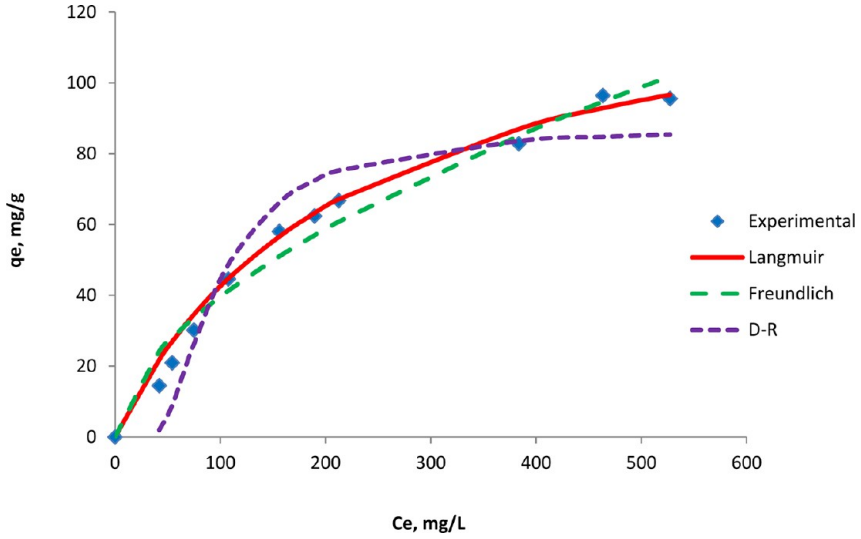

Figure 8. Fitting of experimental values to the Langmuir, Freundlich, and Dubinin−Radushkevich isotherm models for the adsorption of 3,4-di-Cl-Ph onto the 50:50 CS/γ-TCD composite material.

Table 2. Adsorption Isotherm Parameters for the Adsorption of 3,4-Dichlorophenol onto 100% CS and 50:50 CS/γ-TCD Composite Materials

3,4-Dichlorophenol										
	Langmuir Isotherm Parameters			Freundlich Isotherm Parameters			D−R Isotherm Parameters			
	q_{max}(mg/g)	K_L(L/mg)	R^2	n	K_F(mg/g)(L/mg)1/n	R^2	q_{max}(mg/g)	β(mmol^{2}J^{-2})	E (kJ/mol)	R^2
100% CS	63.2	0.0004	0.977	1.0	0.015185	0.970	26.7	0.0805	2.5	0.972
50:50 CS:γ-TCD	137.6	0.0045	0.984	1.4	1.34975	0.949	102.6	0.0026	13.9	0.912

0.984, 0.970 and 0.949, and 0.972 and 0.912, respectively. Relatively good agreement was also found for the saturation adsorption capacity q_{max} values obtained with the Langmuir model and the D−R model: 137.6 and 102.6 mg/g by 50:50 CS/γ-TCD and 63.2 and 26.7 mg/g by 100% CS. The good fit between the Langmuir isotherm model and the experimental data suggests that the sorption is monolayer; the sorption of each molecule has the same activation energy and the analyte−analyte interaction is negligible.[58]

Additional information on the adsorption process can be obtained from the Freundlich isotherm model, particularly from the constant n in eq SI-8 (of the Supporting Information) because it is known to be a measure of the favorability of the sorption process.[58] Because n was found to be 1.0 and 1.4 for 100% CS and 50:50 CS/γ-TCD, respectively, the adsorption of 3,4-dichlorophenol by the latter seems to be more favorable than that of the former.

From the fitting to the Dubinin−Radushkevich isotherm model, the mean free energy E values of the sorption process per mole of 3,4-di-Cl-Ph were found to be 2.5 and 13.9 kJ/mol for 100% CS and 50:50 CS/γ-TCD, respectively. According to this theory (detailed information in the Supporting Information), the sorption of 3,4-di-Cl-Ph onto the 50:50 CS/γ-TCD composite film is chemisorption and is much stronger than that onto 100% CS, which is more by physisorpiton. This finding is as expected because as described above the 50:50 CS/γ-TCD composite material can readily form inclusion complexes with 3,4-dichlorophenol and adsorption by inclusion complex formation is relatively stronger and is chemisorbed by nature compared to 100% CS, which can adsorb the analyte only by surface adsorption.

Taken together, the adsorption isotherm results fully support the kinetic results. Specifically, both sets of results clearly indicate that 50:50 CS/γ-TCD with its ability to form inclusion complexes with 3,4-dichlorophenol can strongly and effectively adsorb much more analyte compared to 100% CS, which can adsorb only by surface adsorption, which is weaker and less effective.

4. CONCLUSIONS

We have successfully developed a novel, simple, one-step method for synthesizing novel, high-performance supramolecular polysaccharide composite materials from CEL, CS, and α-, β-, and γ-TCD. [BMIm$^+$Cl$^-$], an ionic liquid (IL), was used as the sole solvent for the dissolution and preparation of the composites. Because the majority (more than 88%) of [BMIm$^+$Cl$^-$] used was recovered for reuse, the method is recyclable. The [CEL/CS + TCDs] composites that were obtained retain properties of their components, namely, superior mechanical strength (from CEL), an excellent adsorption capability for pollutants (from CS), and the ability to form inclusion complexes selectively with substrates with appropriate sizes and shapes (from γ-TCDs). Specifically, both CS- and TCD-based composite materials can effectively adsorb pollutants such as endocrine disruptors (e.g., chlorophenols and bisphenol A). Although CS-based composites can effectively adsorb the pollutants, its adsorption is independent of the size and structure of the analytes. Conversely, the adsorption by TCD-based composites exhibits a strong dependence on the size and structure of the analytes. For example, whereas all three TCD-based composites (i.e., α-, β-, and γ-TCD) can effectively adsorb 2-, 3-, and 4-chlorophenol, only the γ-TCD-based composite can adsorb analytes with bulky groups

dx.doi.org/10.1021/la3050016 | Langmuir 2013, 29, 5037−5049

including 3,4-dichloro- and 2,4,5-trichlorophenol. Furthermore, equilibrium sorption capacities for the analytes with bulky groups by the γ-TCD-based composite are much higher than those of the CS-based composites. These results together with results from adsorption kinetics and the adsorption isotherm clearly indicate that the γ-TCD-based composite with its relatively larger cavity size can readily form inclusion complexes with analytes with bulky groups, and through inclusion complex formation, it can strongly adsorb many more analytes with a size/structure selective compared to those of CS-based composites that can adsorb the analyte only by surface adsorption. For example, up to 138 mg of 3,4-dichlorophenol can be adsorbed by 1 g of the 50:50 CS/γ-TCD composite material compared to only 63 mg of 3,4-dichlorophenol per 1 g of 100% CS material. Preliminary results presented in this study are very encouraging and clearly indicate that a higher adsorption efficiency can be obtained by judiciously modifying the experimental conditions (e.g., replacing the film of composite materials with microparticles to increase the surface area). Furthermore, because all composite materials used in this study (CEL, CS, CEL + TCD, and CS + TCD) are chiral because of their glucose and glucosamine units in CEL, CS, and TCD, it is expected that they may exhibit some stereospecificity in the adsorption of chiral analytes. These possibilities are the subject of our current intense study.

■ ASSOCIATED CONTENT

Supporting Information

Information on the analysis of kinetic data and equilibrium sorption isotherms. This material is available free of charge via the Internet at http://pubs.acs.org.

■ AUTHOR INFORMATION

Corresponding Author

*Tel: 1 414 288 5428. E-mail: chieu.tran@marquette.edu.

Notes

The authors declare no competing financial interest.

■ ACKNOWLEDGMENTS

Research reported in this publication was supported by the National Institute of General Medical Sciences of the National Institutes of Health under award number R15GM099033.

■ REFERENCES

(1) Katsuhiko, A.; Kunitake, T. *Supramolecular Chemistry: Fundamentals and Applications*; Springer: Berlin, 2006.

(2) Rebek, J., Jr. Introduction to the molecular recognition and self-assembly special feature. *Proc. Nat. Acad. Sci. U.S.A.* **2009**, *106*, 10423−10424.

(3) Rebek, J., Jr. Molecular behavior in small spaces. *Acc. Chem. Res.* **2009**, *42*, 1660−1668.

(4) Hinze, W. L.; Armstrong, D. W. Organized surfactant assemblies in separation science. *ACS Symp. Ser.* **1987**, *342*, 2−82.

(5) Fakayode, S. O.; Brady, P. N.; Pollard, D. A.; Mohammed, A. K.; Warner, I. M. Multicomponent analyses of chiral samples by use of regression analysis of UV-visible spectra of cyclodextrin guest-host complexes. *Anal. Bioanal. Chem.* **2009**, *394*, 1645−1653.

(6) Fakayode, S. O.; Lowry, M.; Fletcher, K. A.; Huang, X.; Powe, A. M.; Warner, I. M. Cyclodextrins host-guest chemistry in analytical and environmental chemistry. *Curr. Anal. Chem.* **2007**, *3*, 171−181.

(7) Kitaoka, M.; Hayashi, K. Adsorption of bisphenol A by cross-linked β-cyclodextrin polymer. *J. Incl. Phenom. Macro. Chem.* **2002**, *44*, 429−431.

(8) Nishiki, M.; Tojima, T.; Nishi, N.; Sakairi, N. β-Cyclodextrin-linked chitosan beads: preparation and application to removal of bisphenol A from water. *Carbohydrate Lett.* **2000**, *4*, 61−67.

(9) Augustine, A. V.; Hudson, S. M.; Cuculo, J. A. *Cellulose Sources and Exploitation*; Ellis Horwood: New York, 1990.

(10) Dawsey, T. R. *Cellulosic Polymers, Blends and Composites*; Carl Hanser Verlag: New York, 1994.

(11) Masanori, Y.; Shinya, T. DNA−cyclodextrin−inorganic hybrid material for absorbent of various harmful compounds. *Mater. Chem. Phys.* **2011**, *126*, 278−283.

(12) Murai, S.; Kinoshita, K.; Ishii, S.; Aoki, N.; Hattori, K. Removal of phenolic compounds from aqueous solution by β-cyclodextrin polymer. *Trans. Mater. Res. Soc. Jpn.* **2006**, *31*, 977−980.

(13) Bordenave, N.; Grelier, S.; Coma, V. Hydrophobization and antimicrobial activity of chitosan and paper-based packaging material. *Biomacromolecules* **2010**, *11*, 88−96.

(14) Rabea, E. I.; Badawy, M. E. T.; Stevens, C. V.; Smagghe, G.; Steurbaut, W. Chitosan as antimicrobial agent: applications and mode of action. *Biomacromolecules* **2003**, *4*, 1457−1465.

(15) Burkatovskaya, M.; Tegos, G. P.; Swietlik, E.; Demidova, T. N.; Castano, A. P.; Hamblin, M. R. Use of chitosan bandage to prevent fatal infections developing from highly contaminated wounds in mice. *Biomaterials* **2006**, *27*, 4157−4164.

(16) Rossi, S.; Sandri, G.; Ferrari, F.; Benferonic, M. C.; Caramella, C. Buccal delivery of acyclovir from films based on chitosan and polyacrylic acid. *Pharm. Dev. Technol.* **2003**, *8*, 199−208.

(17) Jain, D.; Banerjee, R. Comparison of ciprofloxacin hydrochloride-loaded protein, lipid, and chitosan nanoparticles for drug delivery. *J. Biomed. Mater. Res., Part B* **2008**, *86*, 105−112.

(18) Ngah, W. S. W. A. N.; Isa, I. M. Comparison study of copper ion adsorption on chitosan, Dowex A-1, and Zerolit 225. *J. Appl. Polym. Sci.* **1998**, *67*, 1067−1070.

(19) Cai, J.; Liu, Y.; Zhang, L. Dilute solution properties of cellulose in LiOH/urea aqueous system. *J. Polym. Sci., Part B: Polym. Phys.* **2006**, *44*, 3093−3101.

(20) Fink, H. P.; Weigel, P.; Purz, H. J.; Ganster, J. Structure formation of regenerated cellulose materials from NMMO-solutions. *Prog. Polym. Sci.* **2001**, *26*, 1473−1524.

(21) Tran, C. D.; Duri, S.; Harkins, A. L. Recyclable synthesis, characterization, and antimicrobial activity of chitosan-based polysaccharide composite materials. *J. Biomed. Mater. Res., Part A* **2013**, 10.1002/jbm.a.34520.

(22) Tran, C. D.; Lacerda, S. H. P. Determination of binding constants of cyclodextrins in room temperature ionic liquids by near-infrared spectrometry. *Anal. Chem.* **2002**, *74*, 5337−5341.

(23) Han, X.; Armstrong, D. W. Ionic liquids in separations. *Acc. Chem. Res.* **2007**, *40*, 1079−1086.

(24) Tran, C. D. Ionic liquids applications: pharmaceutical, therapeutics and biotechnology. *ACS Symp. Ser.* **2010**, *1038*, 35−54.

(25) Welton, T. Room-temperature ionic liquids. Solvents for synthesis and catalysis. *Chem. Rev.* **1999**, *99*, 2071−2083.

(26) Wasserscheid, P.; Welton, T. *Ionic Liquids in Synthesis*; Wiley-VCH: Weinheim, Germany, 2003.

(27) Baptista, M. S.; Tran, C. D.; Gao, G. H. Near infrared detection of flow injection analysis by acousto-optic tunable filter based spectrophotometry. *Anal. Chem.* **1996**, *68*, 971−976.

(28) Duri, S.; Majoni, S.; Hossenlopp, J. M.; Tran, C. D. Determination of chemical homogeneity of fire retardant polymeric nanocomposite materials by near-infrared multispectral imaging microscopy. *Anal. Lett.* **2010**, *43*, 1780−1789.

(29) Liebert, T. F.; Heinze, T. J.; Edgar, K. J. Cellulose solvents: for analysis, shaping and chemical modification. *ACS Symp. Ser.* **2010**, *1033*, 299−317.

(30) Baxter, A.; Dillon, M.; Taylor, K.; Roberts, G. Improved method for I.R. determination of the degree of acetylation of chitosan. *Int. J. Biol. Macromol.* **1992**, *14*, 166−169.

(31) Domzy, J.; Roberts, G. Evaluation of infrared spectroscopic techniques for analyzing chitosan. *Makromol. Chem.* **1985**, *186*, 1671−1677.

(32) Berth, G.; Dautzenberg, H. The degree of acetylation of chitosans and its effect on the chain conformation in aqueous solution. *Carbohydr. Polym.* **2002**, *47*, 39−51.
(33) Fereira, M. C.; Marvao, M. R.; Duarte, M. L.; Nunes, T.Optimization of the Measuring of Chitin/Chitosan Degree of Acetylation by FT-IR Spectroscopy. *Chitin World, Proceedings of the International Conference on Chitin and Chitosan*, 6th ed.; Gdynia, Poland, 1994; pp 480−488
(34) Fereira, M. C.; Marvao, M. R.; Duarte, M. L.; Nunes, T.; Feio, G. Chitosan Degree of Acetylation: Comparison of Two Spectroscopic Methods (^{13}C CP/MAS NMR and Dispersive IR).*Chitin World, Proceedings from the International Conference on Chitin and Chitosan*, 6th ed.; Gdynia, Poland, 1994; pp 476−479
(35) Hirai, A.; Odani, H.; Nakajima, A. Determination of degree of deacetylation of chitosan by ^{1}H NMR spectroscopy. *Polym. Bull.* **1991**, *26*, 87−94.
(36) Santiago de Alvarenga, E. Characterization and properties of chitosan. *Biotechnol. Biopolym.* **2011**, 91−108.
(37) Percot, A.; Viton, C.; Domand, A. Characterization of shrimp shell deproteinization. *Biomacromolecules* **2003**, *4*, 1380−1385.
(38) Li, B.; Zhang, J.; Dai, F.; Xia, W. Purification of chitosan by using sol-gel immobilized pepsin deproteinization. *Carbohydr. Polym.* **2012**, *88*, 206−212.
(39) Xu, A.; Wang, J.; Wang, H. Effect of anionic structure and lithium salts addition on the dissolution of cellulose in 1-butyl-3-mrthylimidazolium-based ionic liquid solvent systems. *Green Chem.* **2010**, *12*, 268−275.
(40) Xiao, W.; Chen, Q.; Wu, Y.; Wu, T.; Dai, L. Dissolution and blending of chitosan using 1,3-dimethylimidazolium chloride and 1-H-3-methylimidazolium chloride binary ionic liquid solvent. *Carbohydr. Polym.* **2011**, *83*, 233−238.
(41) Fendt, S.; Padmanabhan, S.; Blanch, H. W.; Prausnitz, J. M. Viscosities of acetate or chloride based ionic liquids and some of their mixtures with water or other common solvents. *J. Chem. Eng. Data* **2011**, *56*, 31−34.
(42) Swatloski, R. P.; Spear, S. K.; Holbrey, J. D.; Rogers, R. D. Dissolution of cellulose with ionic liquids. *J. Am. Chem. Soc.* **2002**, *124*, 4974−4975.
(43) Zhang, H.; Wu, J.; Zhang, J.; He, J. 1-Allyl-3-methylimidazolium chloride room temperature ionic liquid: a new and powerful nonderivatizing solvent for cellulose. *Macromolecules* **2005**, *38*, 8272−8277.
(44) Da Roz, A. L; Leite, F. L.; Pereiro, L. V.; Nascente, P. A. P; Zucolotto, V.; Oliveira, O. N., Jr.; Carvalho, A. J. F. Adsorption of chitosan on spin-coated cellulose films. *Carbohydrate Polym.* **2010**, *80*, 65−70.
(45) Dreve, S.; Kacso, I.; Bratu, I.; Indrea, E. Chitosan-based delivery systems for diclofenac delivery: preparation and characterization. *J. Phys.: Conf. Ser.* **2009**, *182*, 1−4.
(46) Burns, D. A.; Ciurczak, E. W. *Handbook of Near-Infrared Analysis*; Marcel Dekker: New York, 1992.
(47) Socrates, G. *Infrared Characteristic Group Frequencies*; John Wiley: New York, 1994.
(48) Bettinetti, G.; Sorrenti, M.; Catenacci, L.; Ferrari, F.; Rosi, S. Polymorphism, pseudopolymorphism, and amorphism of peracetylated α-, β-, and γ-cyclodextrins. *J. Pharm. Biomed. Anal.* **2006**, *41*, 1205−1211.
(49) Ellis, J. W. Infra-red absorption by the N-H bond II in aryl, alkyl and aryl-alkyl amines. *J. Am. Chem. Soc.* **1928**, *50*, 685−695.
(50) Miller, C. E. Chemical Principles of Near-Infrared Technology. In *Near-Infrared Technology: In the Agricultural and Food Industries*, 2nd ed.; Williams, P., Norris, K., Eds.; American Association of Cereal Chemists: St. Paul, MN, 2001; pp 19−37.
(51) Weber, J. W.; Morris, J. C. Kinetics of adsorption of carbon from solution. *J. Sanit. Eng. Div., Am. Soc. Civ. Eng.* **1963**, *89*, 31−39.
(52) Chakraborty, S.; Chowdhury, S.; Saha, P. D. Adsorption of crystal violet from aqueous solution onto NaOH-modified rice husk. *Carbohydr. Polym.* **2011**, *86*, 1533−1541.
(53) Gu, W.; Sun, C.; Liu, Q.; Cui, H. Adsorption of avermectins on activated carbon: equilibrium, kinetics, and UV-shielding. *Trans. Nonferrous Met. Soc. China* **2009**, *19*, 845−850.
(54) Langmuir, I. The constitution and fundamental properties of solids and liquids. *J. Am. Chem. Soc.* **1916**, *38*, 2221−2295.
(55) Freundlich, H. M. F. Over the adsorption in solution. *J. Phys. Chem.* **1906**, *57A*, 385−471.
(56) Dubinin, M. M. The potential theory of adsorption of gases and vapours for adsorbents with energetically non-uniform surfaces. *Chem. Rev.* **1960**, *60*, 235−266.
(57) Dubinin, M. M.; Radushkevich, L. V. The equation of the characteristic curve of the activated charcoal. *Proc. Acad. Sci. USSR Phys. Chem. Sect.* **1947**, *55*, 331−337.
(58) Chowdhury, S.; Chakraborty, S.; Saha, P. Biosorption of Basic Green 4 from aqueous solution by Ananas comosus (pineapple) leaf powder. *Colloids Surf., B* **2011**, *84*, 520−527.